Supporting Information for:

New sensors for quantitative measurement of mitochondrial Zn^{2+}

J. Genevieve Park, Yan Qin, Domenico F. Galati, and Amy E. Palmer

Supplementary Figure 1. Mitochondrial Zn^{2+} sensor design and construction. The mitochondrial targeting sequence (MTS) is cloned into the pcDNA3.1 MCS between HindIII and BamHI. The sensor is flanked by BamHI and EcoRI restriction sites, and the Zn^{2+} binding domain (ZBD) is between SphI and SacI restriction sites. Please refer to Supplementrary Table 1 for primers to amplify the different cpV variants and Supplementary Table 2 for complete amino acid sequences of the ZBDs used in this study.

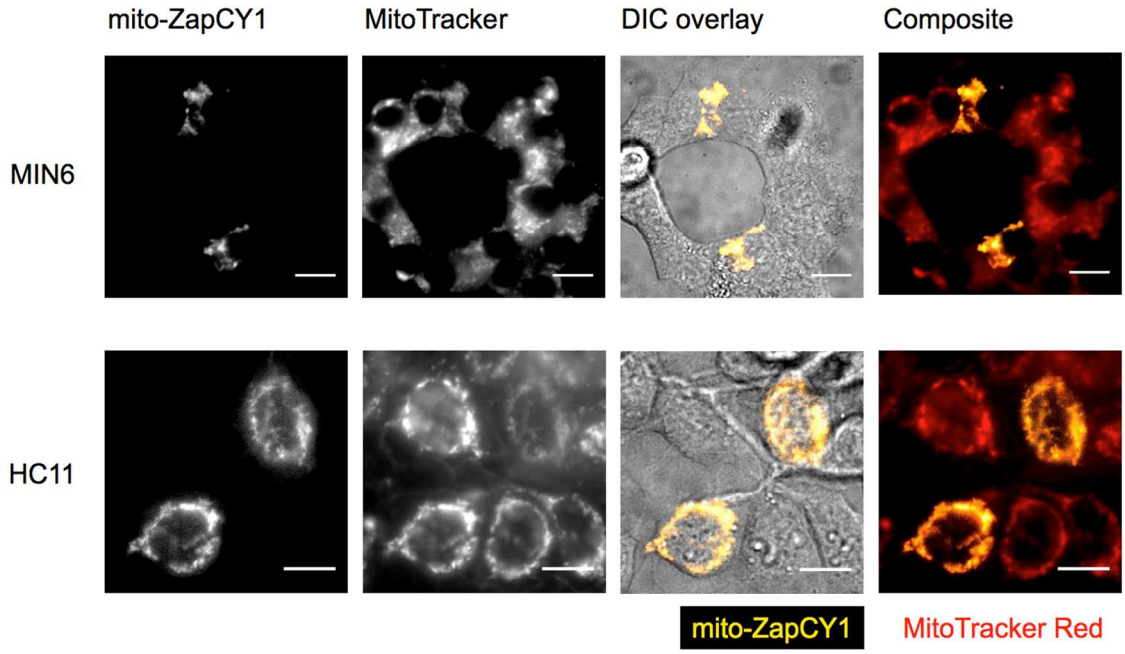

Supplementary Figure 2. Mito-ZapCY1 colocalizes with MitoTracker Red in MIN6 cells and HC11 cells. Cells were transfected with mito-ZapCY1 and imaged 48-72 hours later, and MitoTracker Red dye was loaded into cells 1 hour prior to imaging. Pearson's coefficients for three different images of MIN6 cells are 0.831, 0.563, and 0.88; for two images of HC11 cells are 0.953 and 0.818. Microscope filter combinations for FRET and CFP: 430/24 excitation filter, 455 dichroic, 535/25, and 470/24 emission filters, respectively; for MitoTracker 577/20 excitation filter, 595 dichroic, 630/60 emission filter.

A

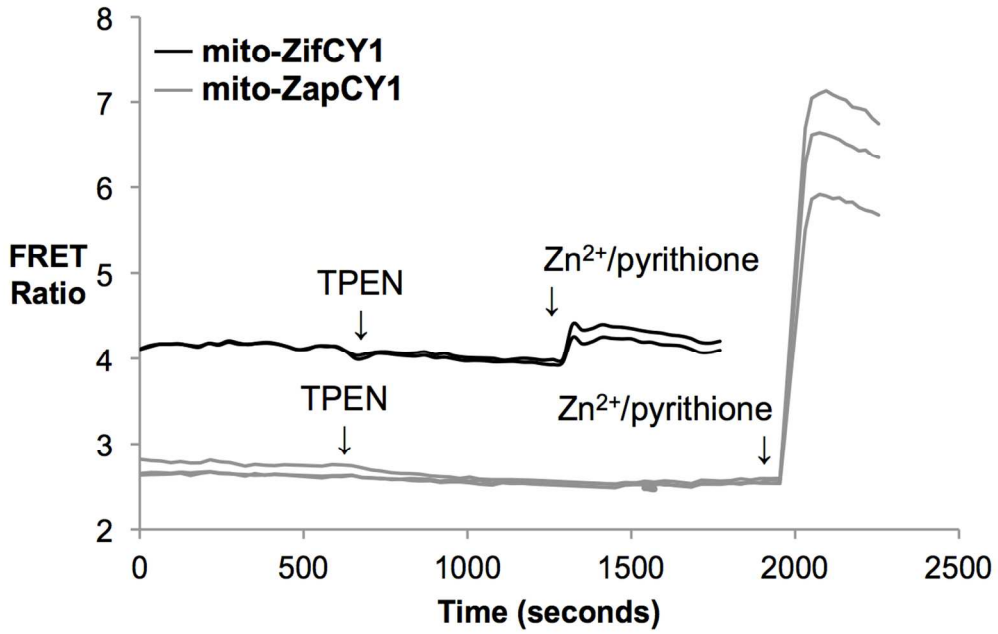

B

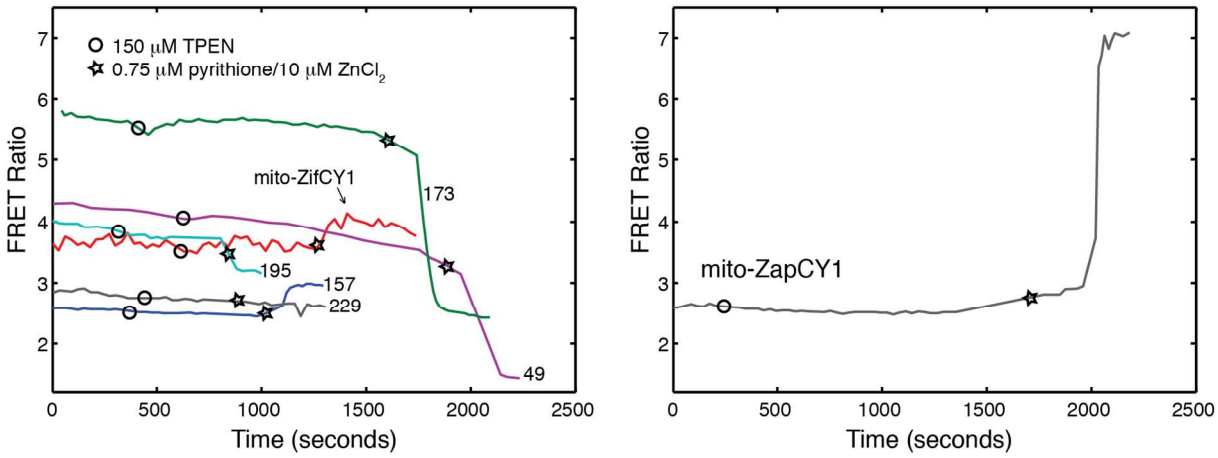

Supplementary Figure 3. Comparison of the dynamic ranges of mitochondrial Zn^{2+} sensors. (A) The dynamic range of mito-ZapCY1 is much greater than that of mito-ZifCY1. Representative calibration traces from HeLa cells expressing either mito-ZapCY1 or mito-ZifCY1 illustrate the significant improvement in dynamic range. 150 μM TPEN was added to reach R_{min}, and 10 μM $ZnCl_2$ and 0.75 μM pyrithione were added to reach R_{max}. (B) Comparison of the dynamic ranges of circularly permuted mito-ZifCY1 variants and mito-ZapCY1. "49" denotes mito-ZifCV1 with Venus circularly permuted at amino acid 49.

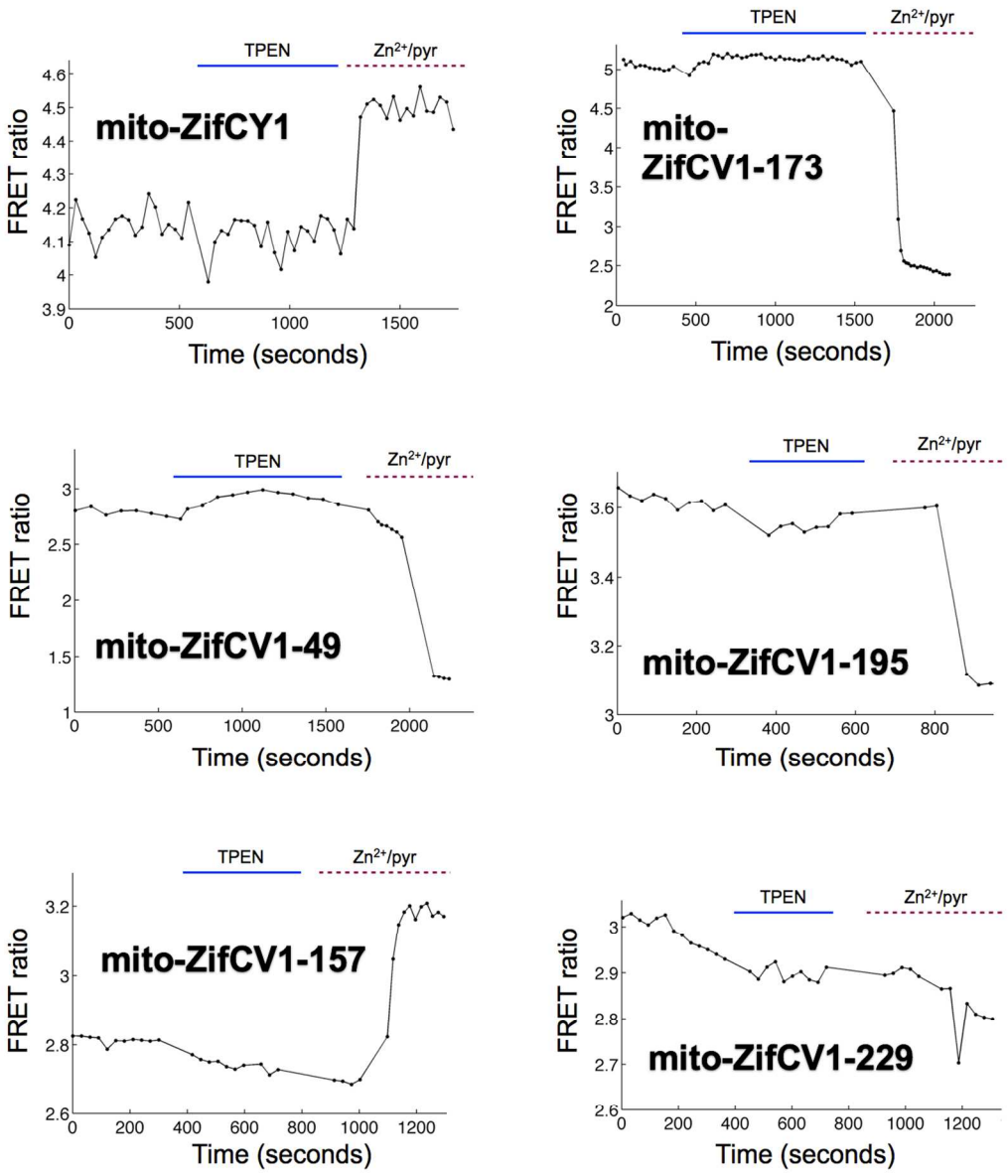

Supplementary Figure 4. Representative calibration traces of mito-ZifCY1 and its circularly permuted variants. 150 μM TPEN was used to deplete Zn^{2+} and 10 μM $ZnCl_2$ and 0.75 μM pyrithione were used to saturate the sensor with Zn^{2+}. FRET ratios differ from those reported in Supplementary Table 3 and Figure 2 due to different exposure times. The mito-ZifCV1.49 and mito-ZifC1.173 calibrations shown above were monitored using shorter YFP FRET exposure times and longer CFP exposure times, resulting in more stable resting FRET ratios, smaller R_{min} and R_{max} but comparable dynamic ranges.

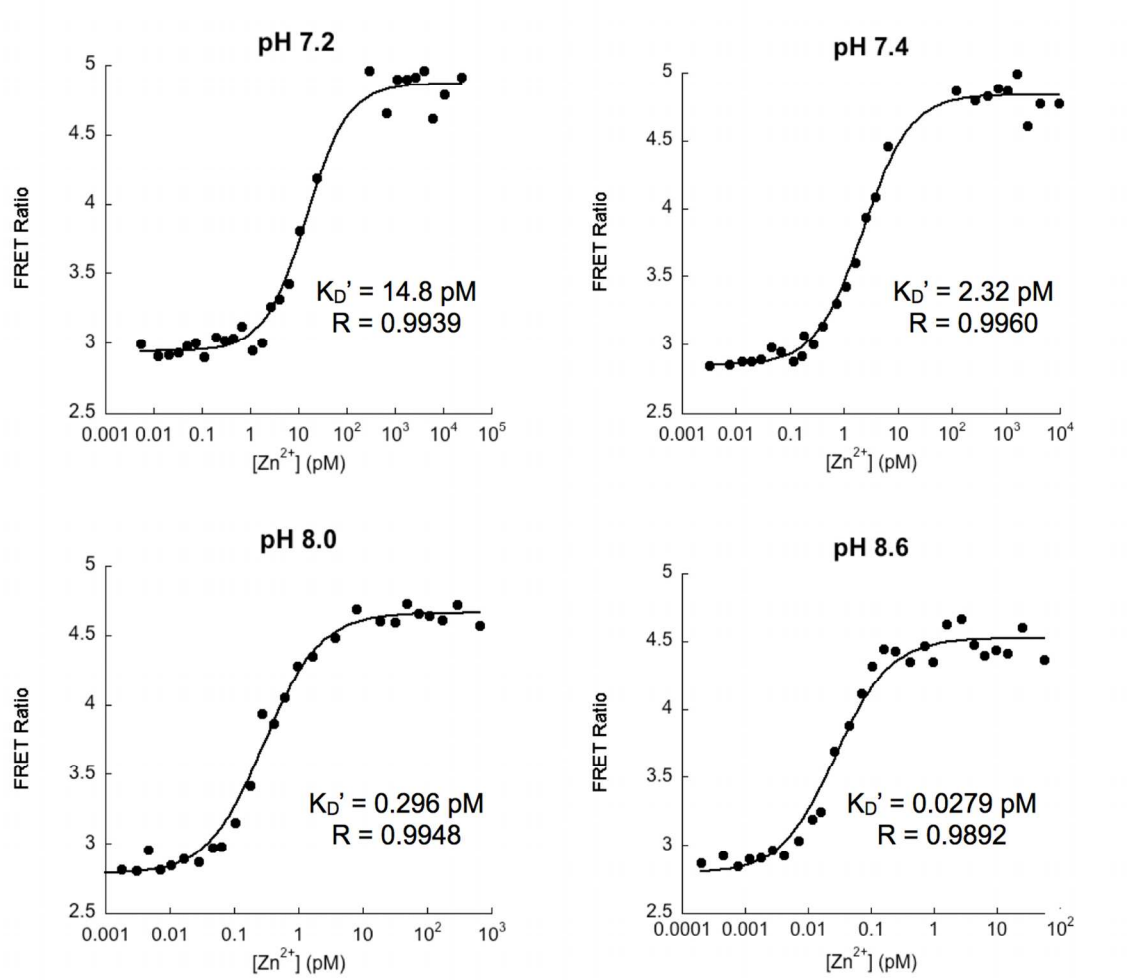

Supplementary Figure 5. The pH dependence of the binding affinity of mito-ZapCY1 *in vitro*. Titrations of the same protein preparation of mito-ZapCY1 were performed *in vitro* at pH 7.2, 7.4, 8.0, and 8.6. Data were fit to a single-site binding equation $R=(R_{max}–R_{min})*[Zn^{2+}]/(K_d'+[Zn^{2+}])+R_{min}$ using the least-squares method in KaleidaGraph software.

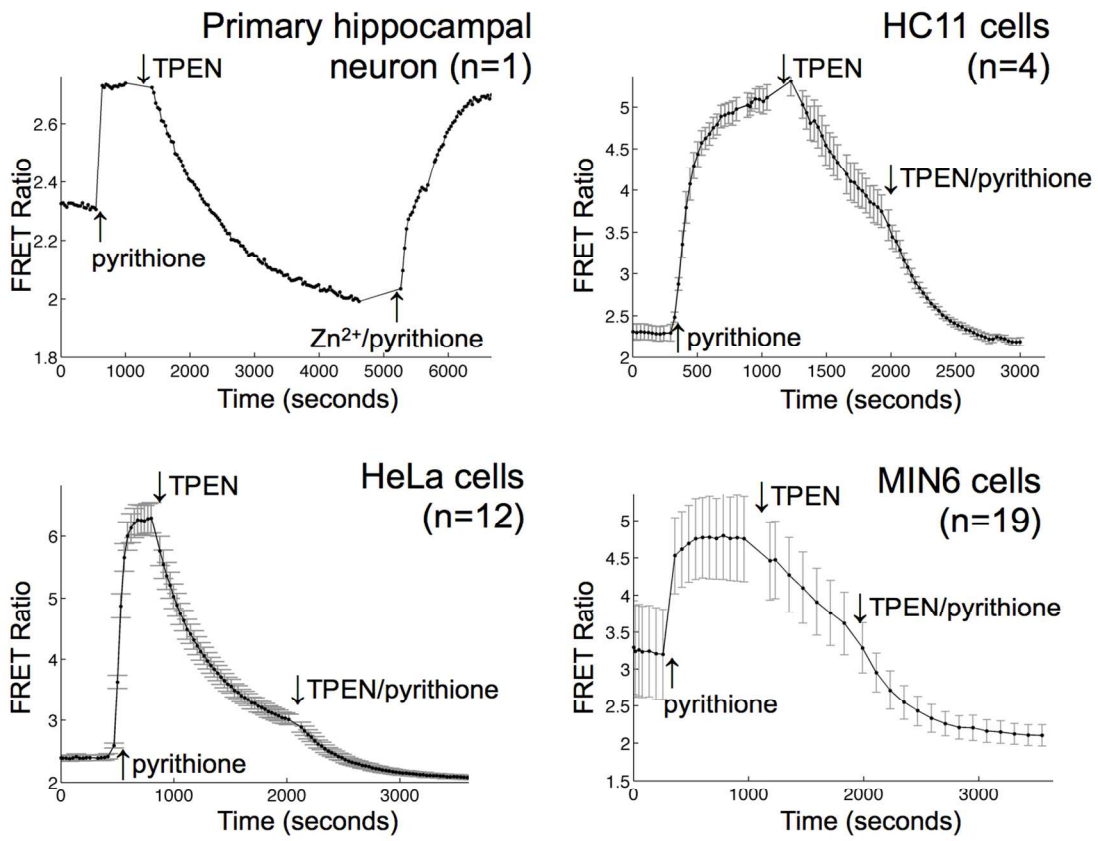

Supplementary Figure 6. Pyrithione treatment alone saturates mito-ZapCY1 in 4 different cell types. Each plot shows the mean +/- the standard deviation of n cells over the course of an experiment. Initially, cells were treated with 5 μM (HC11 and HeLa cells) or 250 μM (neuron and MIN6 cells) pyrithione (pyr). Treatment with 5 μM – 250 μM pyrithione yielded similar results and did not overtly affect cell morphology. Next, the cells were treated with 150 μM TPEN. Finally, cells were treated with 5 μM pyrithione in addition to 10 μM $ZnCl_2$ (neuron) or 150 μM TPEN (all other cells).

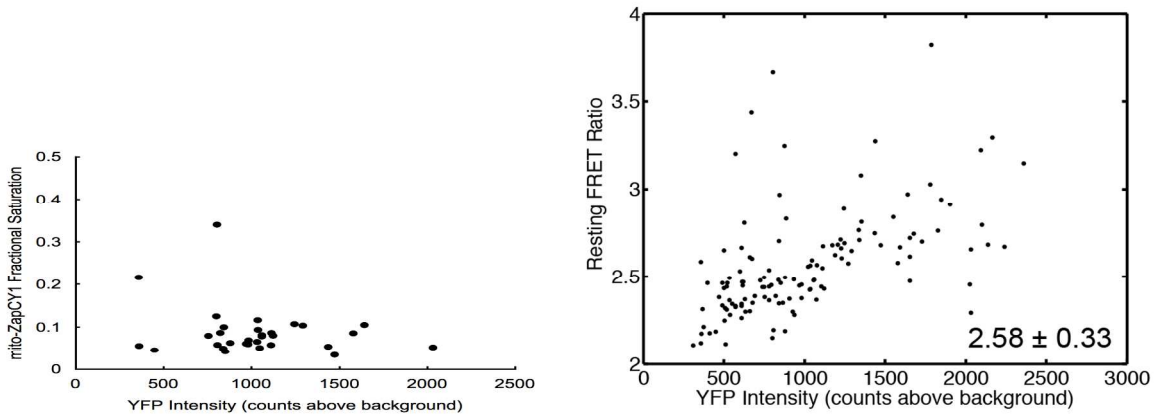

Supplementary Figure 7. The fractional saturation of mito-ZapCY1 does not change as its concentration increases in HeLa cells. Each marker represents a single cell. The YFP intensity is an indicator of sensor concentration because YFP excitation and emission (ex/em) is not affected by FRET. The mito-ZapCY1 resting FRET ratio, in contrast to its fractional saturation, does appear to have some dependence on the YFP intensity, as shown in the right panel.

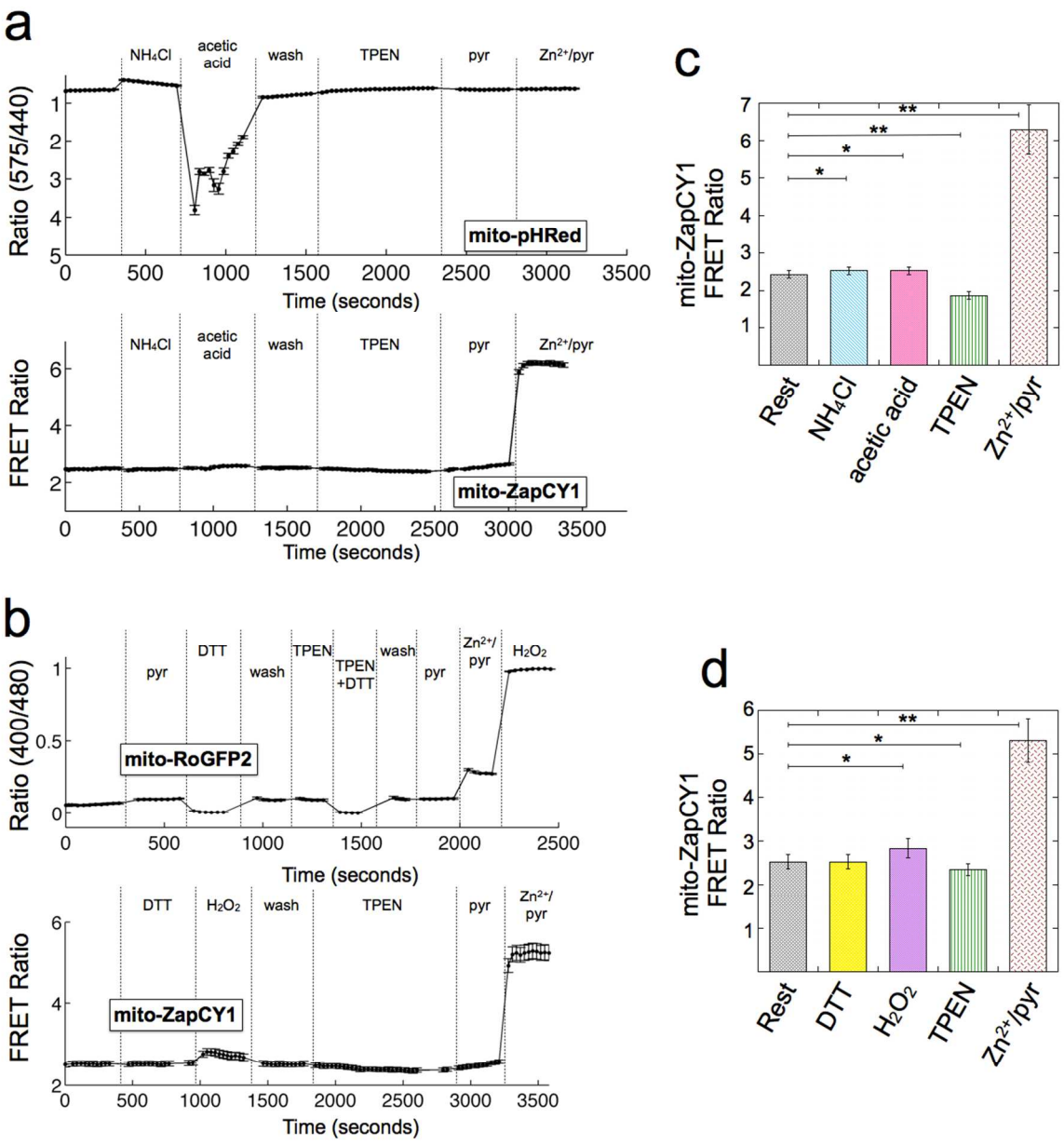

Supplementary Figure 8. The FRET ratio of mito-ZapCY1 is minimally perturbed by changes in pH or redox balance. (a) The FRET ratios of HeLa cells transfected with mito-pHRed or mito-ZapCY1 were measured in the presence of 10 mM NH_4Cl, 10 mM acetic acid, 150 μM TPEN, 250 μM pyrithione, or 10 μM $ZnCl_2$ and 10 μM $ZnCl_2$. (b) The FRET ratios of HeLa cells transfected with mito-RoGFP2 or mito-ZapCY1 were measured in the presence of 250 μM DTT, 250 μM H_2O_2, 150 μM TPEN, or 10 μM $ZnCl_2$ and 250 μM pyrithione. Each plot of FRET ratio over time represents n > 5 cells in a single experiment. Quantification of the FRET ratios (mean ± standard deviation of > 12 cells from at least 2 independent experiments) are shown in (c) and (d) (*$p < 0.05$; **$p < 0.0001$).

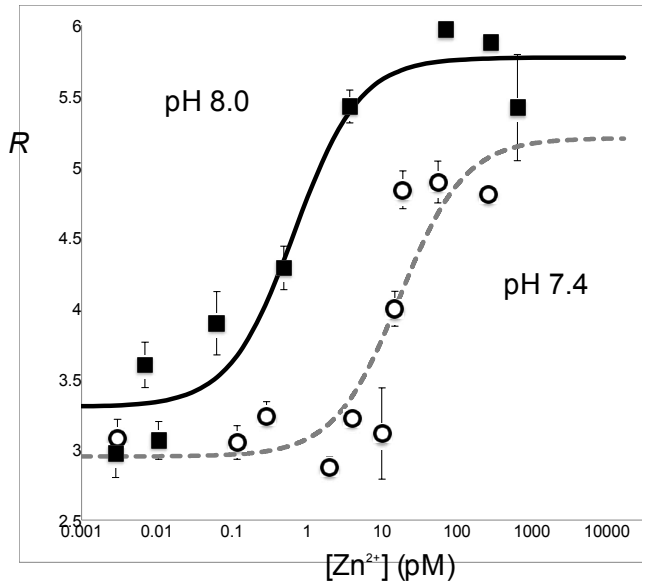

Supplementary Figure 9. Mito-ZapCY1 *in situ* titration data, in terms of FRET ratio R (instead of R–R_{min}). In this analysis, the K_D' of mito-ZapCY1 is 17 pM and 0.68 pM at pH 7.4 and 8.0, respectively.

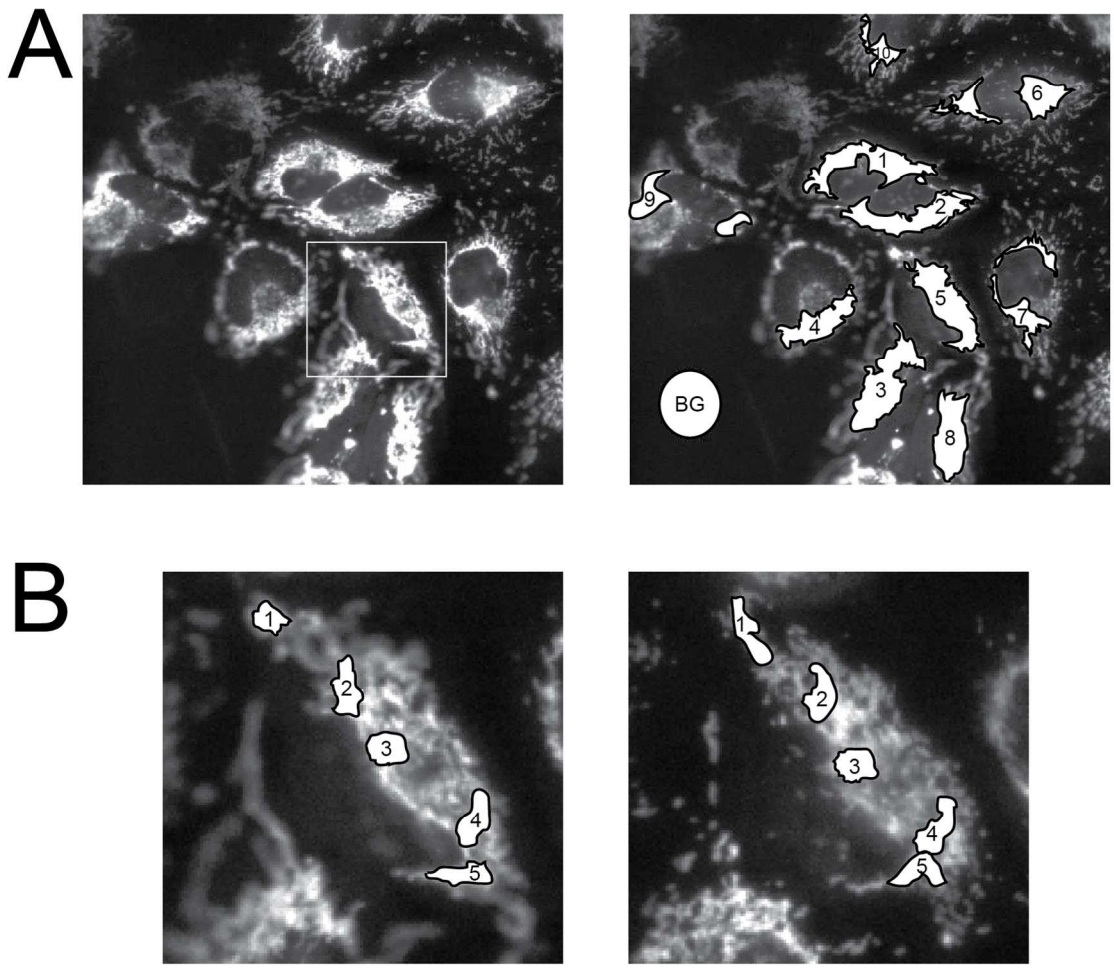

Supplementary Figure 10. Selection of ROIs. One field of view and examples of ROIs selected in that field of view is shown in A. ImageJ was used to calculate the mean intensity of each ROI, including the background (BG) ROI, in the FRET and CFP images. Then, the BG mean intensity was subtracted from each of the other ROIs, and the FRET ratio was calculated as the ratio of the background-subtracted mean FRET intensity to the mean CFP intensity. The results calculated from each cell are presented in Supplementary Table 4. Panel B shows an attempt to select multiple ROIs within cell 5. The image on the left is the first acquisition and the image on the right is the last acquisition. Note that the mitochondria move and change shape throughout the experiment, so it is nearly impossible to track individual mitochondria during an experiment using widefield fluorescence microscopy. The results calculated from each ROI within this cell are presented in Supplementary Table 5.

Supplementary Table 1. Primers used to construct mito-ZifCV1 variants. SacI restriction sites are underlined; EcoRI restriction site is italicized.

Primer name	Sequence (5' to 3')
SacI-cpV49 Fwd	cca<u>GAGCTC</u> ATG ACC GGC AAG CTG CC
SacI-cpV157 Fwd	cca<u>GAGCTC</u> ATG CAG AAG AAC GGC ATC AAG G
SacI-cpV173 Fwd	cca<u>GAGCTC</u> ATG GAC GGC GGC GTG
SacI-cpV195 Fwd	cca<u>GAGCTC</u> ATG CTG CCC GAC AAC CAC
SacI-cpV229 Fwd	cca<u>GAGCTC</u> ATG ATC ACT CTC GGC ATG GAC G
EcoRI-cpV Rev	CAG CCG GAT CAA GCT TC*G AAT TC*T TA

Supplementary Table 2. Amino acid sequences of the different Zn^{2+} binding domains (ZBDs) used in this study. The full sequence of the mitochondrial targeting sequence (MTS) is also shown. Cysteine and histidine residues that ligate Zn^{2+} are colored red and blue, and the 29 amino acid presequence of human cytochrome *c* oxidase subunit 8a is underlined.

ZBD	**Sequence of zinc binding domains**
Zif	ERPYA**C**PVES**C**DRRFSRSDELTR**H**IRI**H**TGQK
TFIIB	MASTSRLDALPRVTCPNHPDAILVEDYRAGDMICPECGLVVG DRVIDVGSEWRTFSNDKATK
MTF1-F345	FECDVQGCEKAFNTLYRLKAHQRLHTGKTFNCESEGCSKYF TTLSDLRKHIRTHTGEKPFRCDHDGCGKAFAASHHLKTHVRT HTGERP
ZapCY1	KNNDLKCKWKECPESCSSLFDLQRHLLKDHVSQDFKHPMEP LACNWEDCDFLGDDTCSIVNHINCQHGI
ZapCY2	KNNDLKHKWKECPESCSSLFDLQRHLLKDHVSQDFKHPMEP LAHNWEDCDFLGDDTCSIVNHINCQHGI
ZapCY3	KNNDLKHKWKEHPESCSSLFDLQRHLLKDHVSQDFKHPMEP LAHNWEDCDFLGDDTCSIVNHINCQHGI
ZapCY4	KNNDLKHKWKEDPESCSSLFDLQRHLLKDHVSQDFKHPMEP LAHNWEDCDFLGDDTCSIVNHINCQHGI
ZapCY5	KNNDLKHKWKEHPESCSSLFDLQRHLLKDHVSQDFKHPMEP LAHNWEDHDFLGDDTCSIVNHINCQHGI
MTS	MSVLTPLLLRGLTGSARRLPVPRAKIHSLGDPMSVLTPLLLRG LTGSARRLPVPRAKIHSLGDPMSVLTPLLLRGLTGSARRLPVP RAKIHSLGDPMSVLTPLLLRGLTGSARRLPVPRAKIHSLGKLG DP

Supplementary Table 3. Characteristics of mitochondrial Zn^{2+} sensors[1] tested.

Sensor name	Zinc binding domain	Donor FP	Acceptor FP	Dynamic Range	Fractional Saturation at Rest	FRET ratio of unbound sensor	FRET ratio of bound sensor	Maximum Ratio - Minimum Ratio	Total # of cells measured	Total # of experiments performed
mito-ZapCY1	Zap	CFP	Citrine	3.22 ± 0.57	0.09 ± 0.06	2.13 ± 0.24	6.78 ± 0.87	4.65	31	3
mito-ZapCY2	Zap mutant #2	CFP	Citrine	1.26 ± 0.01	0.34 ± 0.01	2.26 ± 0.06	2.86 ± 0.09	0.60	6	2
mito-ZapCV2.49	Zap mutant #2	CFP	cpVenus 49	1.16 ± 0.01	0.17 ± 0.05	2.11 ± 0.1	2.45 ± 0.12	0.34	17	1
mito-ZapCV2.173	Zap mutant #2	CFP	cpVenus 173	1.5 ± 0.06	0.04 ± 0.01	3.07 ± 0.2	4.59 ± 0.25	1.52	28	1
mito-ZapCY4	Zap mutant #4	CFP	Citrine	1.13 ± 0.02	0.49 ± 0.14	2.06 ± 0.16	2.33 ± 0.19	0.27	15	1
mito-ZapCY5	Zap mutant #5	CFP	Citrine	1.14 ± 0.04	0.47 ± 0.18	2.04 ± 0.23	2.33 ± 0.2	0.29	18	2
mito-TFIIBCY1	ZF from TFIIB	CFP	Citrine	1.1 ± 0.02	0.89 ± 0.02	2.28 ± 0.21	2.51 ± 0.19	0.23	2	1
mito-MTF35CY1	ZF 3 and 5 of MTF-1	CFP	Citrine	1.13 ± 0.02	0.18 ± 0.11	1.98 ± 0.14	2.23 ± 0.16	0.25	11	2
mito-ZifCY1	Zif	CFP	Citrine	1.17 ± 0.09	0.42 ± 0.27	3.52 ± 0.29	4.24 ± 0.31	0.72	10	3
mito-ZifCV1.49	Zif	CFP	cpVenus 49	2.49 ± 0.38	0.1 ± 0.12	14.2 ± 2.42	5.16 ± 1.26	9.03	16	3
mito-ZifCV1.157	Zif	CFP	cpVenus 157	1.22 ± 0.13	0.16 ± 0.09	2.32 ± 0.23	2.83 ± 0.35	0.51	19	2
mito-ZifCV1.173	Zif	CFP	cpVenus 173	2.56 ± 0.46	0.05 ± 0.08	14.7 ± 4.63	5.35 ± 0.68	9.35	12	2
mito-ZifCV1.195	Zif	CFP	cpVenus 195	1.15 ± 0.04	0.28 ± 0.2	4.01 ± 0.45	3.48 ± 0.35	0.53	14	2
mito-ZifCV1.229	Zif	CFP	cpVenus 229	1.04 ± 0.02	0.42 ± 0.21	3.24 ± 0.57	3.1 ± 0.51	0.14	13	2

[1] For comparison, the recently developed mito-CA probe,[1] which was successfully used to estimate $[Zn^{2+}]_{mito}$ in rat PC-12 cells, is excitation ratiometric (excitation at 360 nm and 540 nm, emission at ~615 nm) and yields a dynamic range of 1.6 and R_{max}–R_{min} of 0.32 in isolated mitochondria. In cells, the ration may vary due to differential loading of the small molecule fluorophore, dapoxyl sulfonamide.

Supplementary Table 4. Mito-ZapCY1 FRET ratios in different cells in one imaging experiment.

Cell #	R_{rest}	R_{free}	R_{bound}	Fractional Saturation	Estimated free $[Zn^{2+}]_{mito}$
1	2.38	1.91	7.05	0.0921	0.162
2	2.42	1.89	5.93	0.131	0.242
3	2.48	1.96	6.82	0.108	0.193
4	2.19	1.76	7.27	0.078	0.136
5	2.48	1.98	6.72	0.107	0.192
6	2.39	1.92	6.20	0.110	0.198
7	2.36	1.83	6.30	0.119	0.217
8	2.60	2.05	6.83	0.115	0.207
9	2.20	1.75	7.16	0.0838	0.146
10	2.16	1.76	4.45	0.150	0.282
Average	2.37	1.88	6.47	0.109	0.198
Standard deviation	0.14	0.10	0.83	0.022	0.044

Supplementary Table 5. Mito-ZapCY1 FRET ratios in different ROIs within one cell.

ROI #	R_{rest}	R_{free}	R_{bound}	Fractional Saturation	Estimated free $[Zn^{2+}]_{mito}$ (pM)
1	2.47	2.09	7.14	0.0745	0.129
2	2.45	2.04	7.01	0.0835	0.146
3	2.49	2.07	6.81	0.0891	0.156
4	2.48	2.03	6.84	0.0937	0.165
5	2.48	2.09	6.91	0.0810	0.141
Average	2.47	2.06	6.94	0.0843	0.147
Standard Deviation	0.01	0.03	0.13	0.0074	0.014

Supporting Methods

Sensor construction

Mito-ZapCY1 was constructed from two previously published constructs: mito-ZifCY1 (renamed from mito-Cys_2His_2; [2]) and ZapCY1 [3], both in the vector backbone pcDNA3 (Life Technologies). Both plasmids were digested with BamHI and EcoRI (NEB), gel-purified, and ligated. Mito-Zif sensor variants were constructed from the ZifCY1 construct in a pBAD vector (a modified vector obtained from R.Y. Tsien) and from cpVenus constructs in the pRSETB vector (Life Technologies). The restriction sites SacI and EcoRI were appended on to the 5' and 3' ends, respectively, of each cpVenus, using PCR amplification. Primer sequences can be found in Supplementary Table 1. pBAD-ZifCY1 was digested with SacI and EcoRI (which removes Citrine from the construct) and each cpVenus was ligated into that plasmid. Then, each pBAD-ZifCV1 construct was digested with BamHI and EcoRI and ligated into the pcDNA-mito vector described above. Refer to Supplementary Figure 1 for a schema of the mito-Zn^{2+} sensors.

Primary cortical neurons

Cerebral cortex was isolated from P0 rat pups, minced with a surgical scalpel and digested with papain for 30 minutes at room temperature. Following digestion, tissue chunks were successively triturated in DMEM supplemented with 10% FBS and pen/strep using a fire polished glass pipet. Neurons were plated onto poly-D-lysine coated 35 mM glass bottom dishes at a density of 250,000 cells cm^{-2} at day in vitro (DIV) 0. At DIV 1, cultures were transferred to Neurobasal A supplemented with B-27

and the antimitotic AraC. At DIV 8, cultures were transfected with 1 μg plasmid (750 ng plasmid of interest/250 ng empty vector) using Lipofectamine 2000.

Cellular imaging.

Cells were plated on 35 mm, glass bottom imaging dishes 24-48 hours before transfection, and imaged 24 to 72 hours after transfection. Before imaging, cells were washed 3 times in phosphate-free HEPES buffered Hank's Balanced Salt Solution (HHBSS), containing 1.26 mM calcium chloride, 5.4 mM potassium chloride, 1.1 mM magnesium chloride, 137 mM sodium chloride, 16.8 mM D-glucose, 20 mM HEPES, pH 7.4, 20-25°C. Phosphate-free HHBSS was used as the imaging buffer except in cases where mitochondria were permeabilized with alamethicin. The following solutions were used for mitochondrial Zn^{2+} calibrations: 150 μM TPEN (25 mM in 100% DMSO stock solution) to remove Zn^{2+} from sensors; 0.75 μM pyrithione (500 □M in 100% DMSO stock solution) and 10 μM $ZnCl_2$ (400 μM in phosphate-free HHBSS stock solution) to saturate Zn^{2+} sensors. During *in situ* titration experiments, the imaging buffer was exchanged to Ca^{2+}-, Mg^{2+}, and phosphate-free HHBSS (phosphate-free HHBSS with calcium chloride and magnesium chloride omitted) immediately before membrane permeabilization with 50 μg/mL alamethicin (10 mg/mL in 100% DMSO stock solution).

Data Analysis.

First, ROIs were manually selected to encompass an area within a cell with dense mitochondria (usually surrounding the nucleus)-see Supplementary Figure 3. A background region was also selected. ImageJ was used to measure the mean intensity of each ROI (in the FRET and CFP images), and then the mean background intensity was subtracted from that value. FRET ratios were calculated as:

$$R = \frac{FRET - BG_{FRET}}{CFP - BG_{CFP}}$$

Next, the FRET ratios were plotted over time. R_{Rest} was the mean R over 5 minutes (10-15 acquisitions). R_{min} was calculated by taking the minimum R before TPEN was washed out, or the decrease in R over time was fit to an exponential decay function to extrapolate R_{min}. R_{max} was the maximum R. If R did not stabilize at R_{max} for more than one acquisition, the data were discarded. Typically, R_{max} was be stable for at least 5 minutes. These values were used to calculate the fractional saturation of the sensor at rest:

$$Fractional\ Saturation = \frac{R - R_{min}}{R_{max} - R_{min}}$$

To convert R to $[Zn^{2+}]$, the following equation [2,3] was used:

$$[Zn^{2+}] = K_D{}' \frac{R - R_{min}}{R_{max} - R}$$

To calculate the Pearson's correlation coefficient, images were cropped to include only one transfected cell. The JACoP[4] plugin for ImageJ[5] (http://rsbweb.nih.gov/ij/plugins/track/jacop.html) was used to calculate the Pearson's coefficient.

References:

(1) Mccranor, B.; Bozym, R. A.; Vitolo, M.; Fierke, C. A.; Bambrick, L.; Polster, B.; Fiskum, G.; Thompson, R. B. (2012) Quantitative imaging of mitochondrial and cytosolic free zinc levels in an in vitro model of ischemia/reperfusion. *J Bioenerg Biomembr.* .

(2) Dittmer, P.; Miranda, J.; Gorski, J.; Palmer, A. (2009) Genetically Encoded Sensors to Elucidate Spatial Distribution of Cellular Zinc. *Journal of Biological Chemistry. 284*, 16289-16297.

(3) Qin, Y.; Dittmer, P. J.; Park, J. G.; Jansen, K. B.; Palmer, A. (2011) Measuring steady-state and dynamic endoplasmic reticulum and Golgi Zn2+ with genetically encoded sensors. *Proc Natl Acad Sci USA. 108*, 7351-7356.

(4) Bolte, S.; Cordelières, F. P. (2006) A guided tour into subcellular colocalization analysis in light microscopy. *J Microsc. 224*, 213-232.
(5) Schneider, C. A.; Rasband, W. S.; Eliceiri, K. W. (2012) NIH Image to ImageJ: 25 years of image analysis. *Nat Meth. 9*, 671-675.